Research Article Vol. 30, No. 13 / 20 Jun 2022 / Optics Express 22687

Optics EXPRESS

Frequency noise stabilisation of a 1550 nm external cavity diode laser with hybrid feedback for next generation gravitational wave interferometry

ANDREW SPENCER,* BRYAN BARR, ANGUS BELL, JOSEPH BRIGGS, ANDREW MINTY, BORJA SORAZU, JENNIFER WRIGHT, AND KENNETH STRAIN

SUPA, University of Glasgow, Glasgow G12 8QQ, United Kingdom
*andrew.spencer@glasgow.ac.uk

Abstract: Longer wavelength lasers will be needed for future gravitational wave detectors that use cryogenic cooling of silicon based test-mass optics. Diode lasers with a 1550 nm wavelength output are potential seed light sources for such a detector, however diode laser devices have a different spectral profile and higher frequency noise than the solid state lasers used in current detectors. We present a frequency stabilisation system for a 1550 nm external cavity diode laser capable of reducing the laser frequency noise to a level of 0.1 $\frac{\text{Hz}}{\sqrt{\text{Hz}}}$ up to 1 kHz with a unity gain frequency of 535 kHz using a hybrid analogue-digital servo with in-loop cancellation of resonant features. In addition, a method of high speed digital filter optimisation and automated design is demonstrated.

1. Introduction

Highly stable low-noise laser systems are required in several areas of modern physics such as optical clocks [1], gravitational wave detection [2,3] atom interferometry [4] and tests of fundamental physics [5]. Solid-state non-planar ring-oscillator (NPRO) lasers [6] with an output wavelength of 1064 nm are used as the gold-standard low-noise light source for many application such as the current generation of ground-based gravitational wave detectors [7,8].

Designs for the next generation of ground-based gravitational wave detectors include many improvements on the current instrumentation including cryogenic cooling of the core optics to reduce thermal noise within the instrument, heavier test masses to reduce low-frequency limiting quantum noise and suspension thermal noise, and subterranean operation to mitigate seismic noise coupling. Operation at cryogenic temperatures requires a suitable cryogenic optical material with some designs favouring silicon due to suitable optical and thermal properties and the availability of sufficiently large substrates to realise the detector designs [9,10]. This requires a corresponding change of laser system to one of a longer wavelength; either 1550 nm [11] or 2 μm [12] due to the absorption spectrum of silicon.

Telecommunication systems typically use 1550 nm lasers with diode and fibre laser devices of low noise and modulation capability widely available. However, such systems can exhibit more noise than solid-state NPRO devices (which are not available at this wavelength) and the practicalities of stabilising a diode laser for precision sensing applications are non-trivial as is explored in this paper.

External cavity diode lasers (ECDL's) are widely available options with low intrinsic intensity noise and the external cavity design provides a level of reduced frequency noise of the output

#459474 https://doi.org/10.1364/OE.459474
Journal © 2022 Received 28 Mar 2022; revised 28 Apr 2022; accepted 2 May 2022; published 7 Jun 2022

Optics EXPRESS

beam in comparison to other diode laser designs with access to internal actuators of the laser output that can be used for stabilisation [13,14].

In this paper we present a stabilised 1550 nm ECDL system that was developed as the light source for a series of cryogenic interferometry experiments in the Glasgow prototype facility for future ground-based gravitational wave detectors using a scheme that combines high-performance electronics and a novel application of high-speed digital filtering.

2. Frequency noise of diode lasers

Laser sources for high-sensitivity applications such as gravitational wave detectors, require multi-stage active frequency stabilisation schemes to reduce the free-running frequency noise of the laser to the levels required for precision interferometry [15]. The frequency range for detecting gravitational waves with current ground-based detectors is between 10 Hz and 1 kHz, with future detectors such as the Einstein Telescope aiming to push down to 1 Hz for earlier detection of compact binary sources and detection of heavier systems [16]. The laser frequency noise for such an application is required to be stabilised across this band and up to higher frequencies in order to ensure stable operation of the multiple optical cavity locking control schemes employed. The lower frequency limit for gravitational wave detection in ground-based laser interferometers is primarily due to environmental coupling and technical noise limits, meaning below this measurement frequency laser frequency noise is not a primary limitation to the instrument although reduction of the laser free-running noise is required.

In switching to diode lasers, meeting these requirements will be even more demanding as diode lasers typically exhibit higher frequency noise levels with a flatter spectral profile at high measurement frequencies. A comparison of the typical free-running frequency noise in an NPRO versus an ECDL is shown in Fig. 1. For this work demonstrating the first stage of laser frequency stabilisation for future cryogenic interferometry experiments in our prototype facility the target was to have the laser frequency noise reduced to 0.1 $\frac{\text{Hz}}{\sqrt{\text{Hz}}}$ between 100 Hz and 1 kHz.

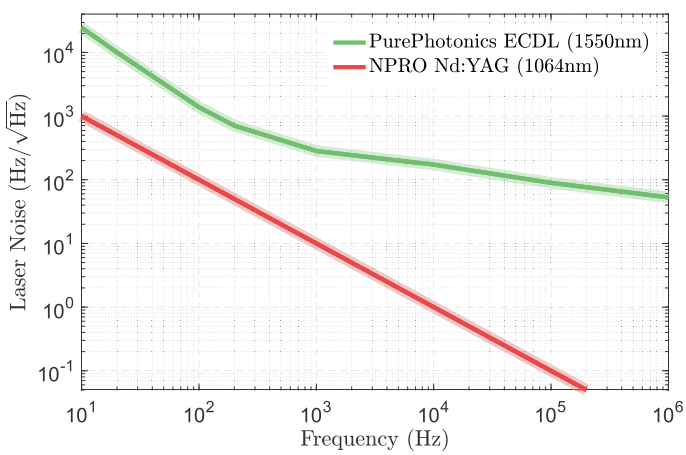

Fig. 1. Comparison of typical free-running frequency noise of a diode laser system (green) [17] and a solid-state NPRO (red) [18]. The shape of the green trace is typical of the noise profile of a diode laser, the noise level and inflection point varies between laser systems.

Broadly speaking, the ECDL frequency noise consists of two features; an approximately 'white' noise source at higher frequencies due to statistical spontaneous emission (higher light intensity in the lasing medium reduces this effect as stimulated emission begins to dominate [19]) and a $1/f$ component at lower frequencies due to current leakage and strain in the semiconductor material itself [20]. The latter effect was for many years poorly understood as it is slightly non-intuitive

Optics EXPRESS

and has thus been investigated in great detail more recently [21]. A qualitative understanding is that electrical carriers (leakage current) passing through a semiconductor will encounter 'trap' points within the material due to defects and Brownian motion. The statistical time delay for these carriers passing through the material will thus result in a $1/f$ fluctuation in the number of carriers (current) in the material.

In semiconductor lasers the refractive index of the gain medium varies with carrier density, so the optical path length (and thus laser cavity length) will vary accordingly. The result is a direct coupling of current fluctuation to laser frequency fluctuations.

For NPRO laser stabilisation a great deal of success has been achieved by direct feedback to the laser cavity optical length to stabilise the laser frequency to a rigid reference cavity [15]. In such systems the main limitations are generally the stability of the reference and dynamic range of the feedback elements, so in the case of an ECDL (even considering the higher initial noise profile) one would expect similar limitations.

3. Frequency stabilisation of a 1550nm ECDL

The 1550 nm laser system consists of an ECDL from Pure Photonics [17] with an output power of 50 mW and frequency and intensity actuators internal to the laser module, this is used to seed a fibre amplifier to produce 5 W of laser power at 1550 nm. For the frequency stabilisation scheme described in this section 8 mW of light is picked off from the main beam, with the remaining optical power available as stabilised probe light for other experiments.

The resonant frequency of the ECDL lasing cavity can be controlled with a PZT length actuator on the external cavity mirror and by temperature control of an intra-cavity etalon filter. The laser frequency can be modulated by driving a voltage across the cavity PZT and the laser intensity can be modulated by varying the current driven through the InP gain chip. It should be noted that the current modulation strongly actuates both laser intensity and frequency [22] while the PZT drive produces almost pure frequency modulation.

The module allows for modulation of the laser output by application of an external control signal to either the laser cavity PZT or the diode current (the temperature actuator could be set to control the output wavelength but could not be directly modulated). Using the PZT actuator for frequency control and the current for intensity allows for actuation, and thereby stabilisation, of two of the lasers output parameters.

3.1. Stabilisation scheme

The stabilisation scheme for the 1550 nm laser is shown in Fig. 2. The laser is locked to a 22 cm long rigid reference cavity with a finesse of 330, that is held under vacuum on a passive seismic isolation platform. The linear optical cavity is formed by two fused-silica mirrors bonded to a Zerodur [23] spacer.

A Pound-Drever-Hall (PDH) locking scheme [24] is used to generate an error signal that is subsequently shaped by an analogue servo and applied to two laser frequency actuators. For frequencies from 10 Hz to 10 kHz the laser cavity PZT provides the actuation, while above 10 kHz a fibre coupled electro-optic modulator (EOM) external to the laser module is used for actuation at these higher frequencies and to avoid feedback to the laser PZT at frequencies close to mechanical modes of the laser module. The EOM is a phase modulator and therefore produces a frequency actuation proportional to the modulation frequency. Thus it is suitable for high frequency feedback but the reduced actuation strength in combination with the increased frequency noise at lower frequencies meant it could not be used to stabilise the laser below 10 kHz.

A high speed digital filter implemented on a field programmable gate array (FPGA) is used in-line in the PZT feedback path to correct for these resonance features in a process that will be discussed in Section 4. This was not actively in use for the results presented in this section.

Optics EXPRESS

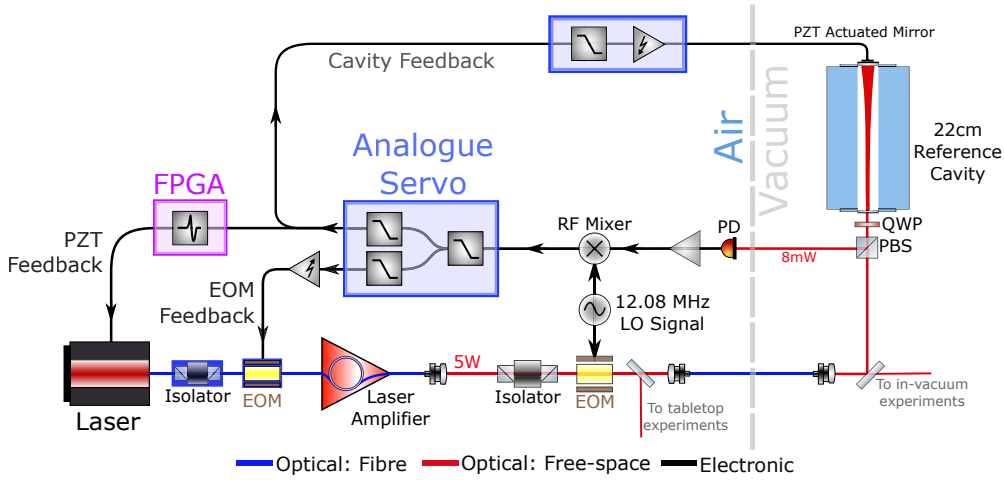

Fig. 2. Frequency stabilisation scheme for the 1550 nm laser system. The laser output is phase modulated by a 12.08 MHz local oscillator (LO) signal applied to a resonant electro-optic modulator (EOM). The beam is fibre coupled into the vacuum system and aligned to a rigid reference cavity. The beam is directed by polarisation beamsplitter (PBS) and quarter-waveplate (QWP) and detected with a broadband photodiode (PD), the AC coupled output of which is amplified before being demodulated with the local oscillator to produce the error signal that is filtered by an analogue servo (blue box) and fed back to multiple frequency actuators. An additional digital filter stage (pink box) is implemented on a field programmable gate array (FPGA) in the feedback to the laser PZT. For wide bandwidth control, both an in-fibre EOM and an internal PZT actuator are used for laser stabilisation, while feedback to the cavity length at low frequencies is used to hold the cavity on resonance.

Due to slow drifts of the laser output frequency, that are greater than the range of the PZT actuator, a scheme is used to improve the long-term stability of the system where a part of the feedback signal is picked off and after additional low-pass filtering is applied to a PZT that actuates the length of the reference cavity. This means that at low frequencies (<1 Hz) the length of the cavity is locked to the frequency of the laser but above this the laser is stabilised to the reference cavity with a separation between laser and cavity feedback of 30 dB at 10 Hz and 70 dB at 100 Hz.

3.2. Results

The results of the laser frequency stabilisation are shown in Fig. 3 as the in-loop noise spectrum and in Fig. 4 as the open loop transfer function of the laser locking loop. The analogue servo for frequency stabilisation contains an injection point at the input stage, a fixed gain, low-pass, summing amplifier with a monitor point at its output. The noise measurements were made as FFT's of the monitor point signal converted to a error point frequency noise spectrum by knowledge of the servo electronics and the slope of the error signal calibrated against the phase modulated control side-bands. The transfer functions were measured by injecting a swept-sine signal into the injection point and measuring the response at the monitor point with the loop closed and converted to an open loop transfer function with knowledge of the electrical response. The free-running noise was inferred from a previous measurement of the in-loop noise and the loop response transfer function and found to be with a factor of two of the specification for the laser (green traces in Fig. 3).

Optics EXPRESS

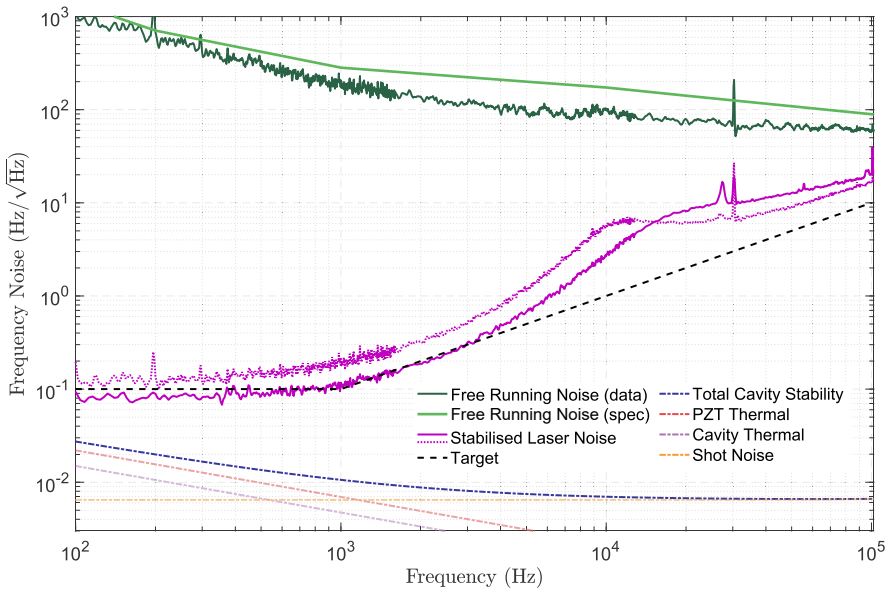

Fig. 3. In-loop measurement of stabilised laser frequency noise amplitude spectral density (ASD) (pink) with respect to the free-running laser frequency noise ASD as measured and corrected for loop response (dark green) and as expected from the manufacturer specification (light green). Two measurements of the stabilised noise are shown with different servo configurations. The noise level was measured, with a spectrum analyser with maximum range of 102 kHz, at the error point of the stabilisation loop locking the laser to the reference cavity. The noise target (black dashed) is shown as determined by the stability required for future cryogenic interferometry experiments within our prototype facility and is clearly above the stability limit of the reference cavity, shown in the dot-dash lines and as discussed in Section 3.2

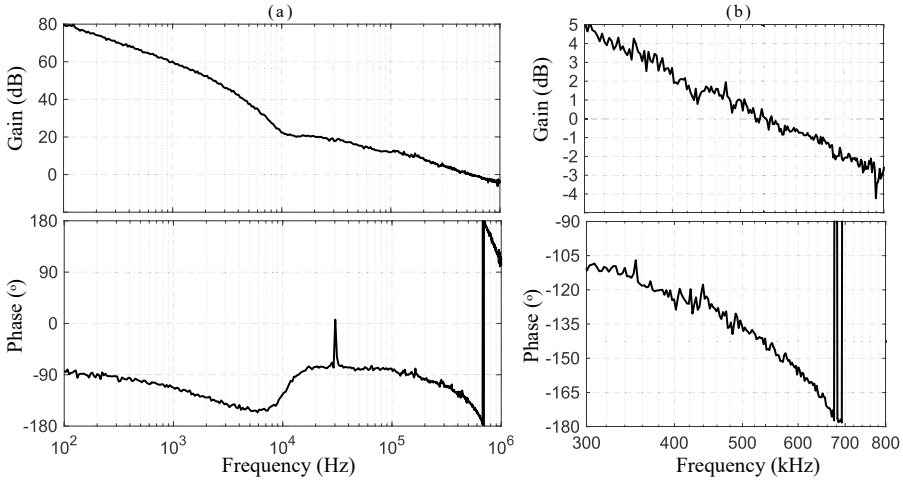

Fig. 4. Open loop transfer function of laser frequency stabilisation loop. The broadband transfer function is shown in (a) and a zoomed in plot is shown in (b) to highlight the stability around the unity gain frequency of 535 kHz with a phase margin of 36°.

Optics EXPRESS

In Fig. 3 two traces of the in-loop stabilised noise spectrum are shown for different configurations of the analogue servo to achieve different shaping of the crossovers between PZT and EOM feedback around 10-20 kHz. In the solid pink trace the target (black dashed) noise level of 0.1 $\frac{\text{Hz}}{\sqrt{\text{Hz}}}$ is met up from 100 Hz to 1 kHz. The target is based on the future requirements of the laser system as a seed for cryogenic interferometry experiments within our prototype facility and the expected length noise stability of the reference cavity. The measured noise can be seen to bulge above the target noise level between 8-30 kHz due to imperfect stability of the feedback crossover. Spikes in the laser noise around 27 kHz and 30.3 kHz are due to mechanical resonances in the laser module that are described in Section 4. At 100 Hz the free-running laser noise is reduced by 80 dB as measured in-loop.

The stabilisation limit of such a scheme is limited by the absolute frequency stability of the reference - in this case the 22 cm optical reference cavity. The stability of such an optical reference is well understood [25] and the cavity used in this work will be limited on the timescales of interest by the thermal noise of the PZT element bonded between spacer and mirror which is expected to have a stability of $2.5 \times 10^{-17} \times (100/f)^{1/2} \frac{\text{m}}{\sqrt{\text{Hz}}}$ [26] which is a factor of 1.5 above the thermal noise of the spacer and mirrors [27] and a factor of 3.6 higher than the shot noise limit of the cavity [28] at 100 Hz. These length stability limits for the reference cavity are plotted in terms of frequency noise (using the relation $\frac{\delta L}{L} = \frac{\delta f}{f}$) as dot-dash lines in Fig. 3. The measured signal was a factor of 10 above the electronic noise floor of the servo and measurement systems. Therefore we can infer that the stabilisation loop is not adding noise onto the laser and is stabilising the laser noise to a level that can be measured in-loop above the stability limit of the cavity. Decreasing the noise (as measured in-loop) further would not decrease the out-of-loop noise of the laser beyond the frequency stability of the cavity.

The open loop transfer function of the laser stabilisation loop is shown in Fig. 4 where the unity gain frequency is 535 kHz with a phase margin (minimum phase change that would produce instability) of 36° and gain margin (minimum gain change that would produce instability) of 2 dB, where instability occurs for a phase lag of −180° concurrent with a open loop gain of 0 dB.

4. Resonant features in the laser frequency noise spectrum

Resonance features related to the laser cavity PZT actuator have a destabilising effect on the servo loop as they happen to lie close to the crossover between the PZT and EOM feedback paths and the magnitude of the noise peaks and the profile in the loop transfer functions change depending on the crossover set-point. Several peaks associated with mechanical back-action resonances internal to the module were observed in the loop response and can be seen in the in-loop noise measurement at 27 kHz and 30.3 kHz in Fig. 3, in the open loop transfer functions in Fig. 4 and in more detail in the measurements in Fig. 5.

If the PZT actuated mirror inside the laser cavity is considered as a mass on a spring, then the back-action resonances can be understood as acoustic oscillations propagating within the structure of the laser module and reflecting from multiple material interfaces. The fundamental resonance of the PZT is at ∼130 kHz but these additional features introduce resonances into the control loop and limit the usable bandwidth of the laser PZT as a linear frequency actuator.

Attempts were made to reduce the impact of these resonances with mechanical damping. The laser module was mounted on a aluminium base-plate which was separated from the laser bench by a layer of damping tape between the aluminium plate and a copper board. This provided a level of constrained layer damping [29] that partially damped the resonance and improved the stability of the laser PZT locking loop but did not remove the resonances.

Optics EXPRESS

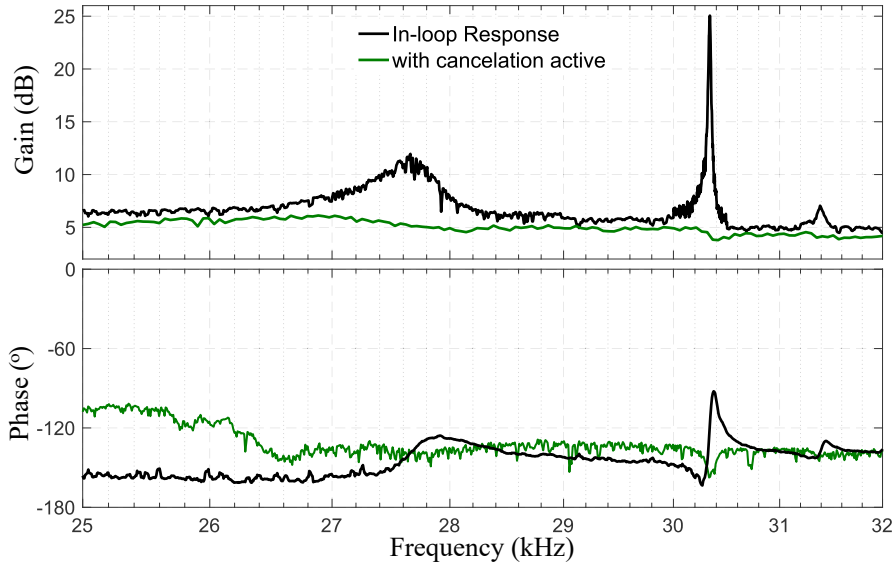

Fig. 5. Transfer function measurements of the laser locking loop between 25 kHz and 32 kHz measured from injection point to monitor point without conversion to open loop response, showing the cancellation of the PZT resonances of the laser with a digital filter. The green trace shows the result of implementing a digital filter designed to cancel out the resonant features seen in the loop response transfer function (black trace).

4.1. Cancellation of resonant features with digital filtering

A method was implemented to cancel the resonate features in the laser stabilisation loop using a fast digital filter implemented on a FPGA device in-line with the feedback to the laser PZT. The device is has a sample rate of 125 MHz and a 14-bit ADC. Such an approach has previously been shown to be effective [30].

The digital filter was designed by recording a high-resolution transfer function of the resonant features, a measurement made with the FPGA, and mathematically fitting pole-zero pairs to this measurement. The result was inverted and used as a cancellation filter. Such an approach is possible because the resonances were minimum phase features. The designed filter was deployed on an FPGA digital signal processing platform placed in-line with the PZT feedback path between the analogue servo and the laser.

For this method to work accurate characterisation of the resonant features is critical. A swept sine measurement is used to generate results such as the black trace in Fig. 5. Driving too large a signal into the loop leads to inaccurate characterisation of the shape of the features and underestimation of the magnitude of the resonant peaks as the energy is spread across the resonant frequencies, leading to incomplete suppression.

The result of this cancellation process is shown in Fig. 5 where the three resonant features at 27.7, 30.3 and 31.4 kHz are suppressed by the filter. The in-loop magnitude of the resonance at 30.1 kHz is reduced from a 20 dB peak to feature on the order of 1 dB.

5. Optimised design of digital filters

Implementing digital filters, on an FPGA or similar device, as series combination of second-order-sections (SOS) [31] allows for a high level of design complexity and tunability. Each SOS contributes two complex poles and two complex zero pairs to the overall transfer function. Each pole or zero can be uniquely defined by a complex number or by a frequency and a Q-factor, and

Optics EXPRESS

it is these filter coefficients that define the filter shape, with a Q-factor of 0.5 corresponding to a first order filter and higher values producing resonant second order filters.

The flexibility of implementation and complexity of design offered by digital filtering leads it be attractive to the application of fast frequency stabilisation of diode lasers. The use of such a high speed digital filter used in combination with an analogue servo was shown in Section 4.

What is presented in this section is a servo design algorithm that allows for the full automation of filter design and optimisation from minimal starting specifications that was used to design filters for a fully digital stabilisation of the 1550 nm diode laser but can be adapted to multiple purposes.

5.1. Filter optimisation algorithm

The design algorithm combines two elements; a Monte-Carlo style random filter generation and a particle swarm optimisation [32,33]. This was done as an off-line process and the parameter later used to implement the filter on a digital platform.

A large number of filters with randomised pole-zero coefficients are generated and a gain factor is set so that a target unity gain frequency (UGF) of the open loop transfer function is possible. From this starting population a down-selection based on a filter quality metric picks out a number of best-case filters to be optimised.

The second-stage optimisation involves generating a population of particles (each representing a filter option) that take the pole-zero values of the starting filter as the seed for a swarm optimisation. In each step of the swarm optimisation each particle is judged against the metric and then assigned a impulse vector based on the location of the best-judged particle in the parameter space (with an element of random walk included) so that on subsequent rounds the particles move though the parameter space and converge at the optimal parameters. In this way an optimal solution to a multi-dimensional parameter space problem can be found. The Monte-Carlo part of the algorithm ensures that local minima of sub-optimal solutions are avoided and the particle swarm vastly speeds up the multi-dimensional Monte-Carlo process by taking the most optimal randomly generated parameters from a set and optimising further while removing the need to sample the whole parameters space either randomly or sequentially.

The metric by which filters are judged is critical to the success of this technique. For a stabilisation filter the important elements are the unity gain frequency, the phase and gain margins for stability and the level of noise reduction. The noise suppression gain from low frequency to the high-gain corner frequency was combined with the phase and gain margin to define the filter figure of merit. This metric included thresholds for what was tolerable in terms of stability and optimal performance.

5.2. Results

An example result of the automated filter design algorithm is shown on Fig. 6. A filter was designed for use in the stabilisation scheme presented in Section 3. to replace the analogue servo (see Fig. 2) for feedback to the laser PZT. The arbitrary goal created to test the algorithm was to design a filter with a flat gain profile with 80 dB of noise suppression up to a corner frequency of 1 kHz and a shape drop-off to a stable unity gain crossing at 10 kHz using four complex pole-zero pairs.

This result achieves an 80 dB gain drop across one frequency decade with a 58° phase margin and 7 dB gain margin. The unity gain frequency of such a filter could be increased to any reasonable frequency, being limited only by the speed of the digital processor and any phase delay in the stabilisation loop.

Given that this system can be broken down into numerical poles and zeros, and can be implemented on any sufficiently fast digital signal processor, it is possible to use such an algorithm in a range of applications of automated filter design and implementation. By

Optics EXPRESS

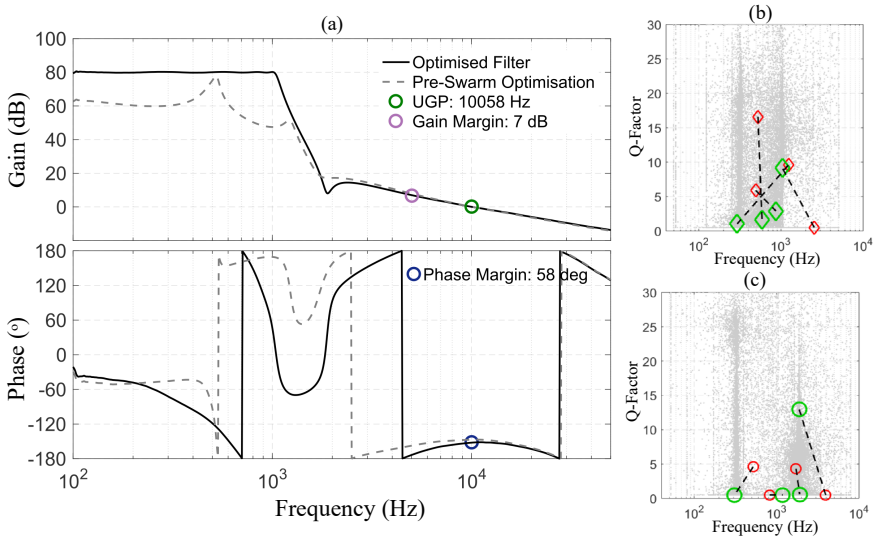

Fig. 6. Automated design of a digital stabilisation filter using swarm optimisation algorithm. The specification was for a UGF at 10 kHz and a flat gain of 80 dB up to the corner frequency of 1 kHz. In this filter four pole-zero pairs were utilised. The modelled open-loop transfer function (a) is shown for the optimised filter implemented in the laser stabilisation scheme, shown in Fig. 2 to replace the analogue servo. The initially selected randomly generated filter (gray dashed) result is shown along with the swarm optimised filter (black). The optimisation process is represented in the parameter spaces in (b) for the poles and (c) for the zeros with each (gray) point a filter considered in the particle swarm along with the initial (red) and final (green) pole-zero coefficients.

automatically analysing a measured noise level (either as an initial off-line characterisation or in real time) and generating an appropriate feedback filter which would then be implemented in digital form, this approach can be used to realise fully automated smart design and application of a complete stabilisation filter or for cancellation of unwanted features in a hybrid analogue-digital control loop such as the one considered in Section 4.

6. Conclusions

The use of diode laser systems as light sources for high-sensitivity experiments presents a certain challenge for frequency noise stabilisation due to the noise spectrum of such devices. In this paper we presented a frequency stabilisation system for a 1550 nm ECDL with a bandwidth of 535 kHz and in-loop noise level of 0.1 $\frac{\text{Hz}}{\sqrt{\text{Hz}}}$ between 100 Hz and 1 kHz, which is a reduction of the free-running noise of 80 dB at 100 Hz as is required for the high-sensitivity interferometer prototype experiments for next generation cryogenic gravitational wave detectors.

Internal resonances of the lasing cavity where shown to be an issue inherent with some ECDL's, creating problematic non-linear features in the control loop that limited the performance of the noise stabilisation system. This was solved with use of a cancellation filter realised on a FPGA fast-digital processor.

The use of digital filters in control schemes is a powerful and flexible tool, the usefulness of which was demonstrated in this paper for the case of resonance cancellation, and the automated design and optimisation of stabilisation filters. This presents a way forward for future work with cryogenic interferometry and other high sensitivity laser applications at this wavelength.

Funding. Science and Technology Facilities Council (1653071, ST/N005422/1).

Optics EXPRESS

Acknowledgements. This work was supported by the Science and Technology Facilities Council (Grant ref: ST/N005422/1) and A. Spencer was supported by STFC Studentship award number 1653071. This paper has LIGO document number P2000321.

Disclosures. The authors declare no conflicts of interest.

Data availability. Data underlying the results presented in this paper are not publicly available at this time but may be obtained from the authors upon reasonable request.

References

1. M. Takamoto, F.-L. Hong, R. Higashi, and H. Katori, "An optical lattice clock," Nature **435**(7040), 321–324 (2005).
2. J. Aasi, B. P. Abbott, R. Abbott, T. Abbott, M. R. Abernathy, K. Ackley, C. Adams, T. Adams, P. Addesso, R. X. Adhikari, V. Adya, C. Affeldt, N. Aggarwal, O. D. Aguiar, A. Ain, P. Ajith, A. Alemic, B. Allen, D. Amariutei, S. B. Anderson, W. G. Anderson, K. Arai, M. C. Araya, C. Arceneaux, J. S. Areeda, G. Ashton, S. Ast, S. M. Aston, P. Aufmuth, C. Aulbert, B. E. Aylott, S. Babak, P. T. Baker, S. W. Ballmer, J. C. Barayoga, M. Barbet, S. Barclay, B. C. Barish, D. Barker, B. Barr, L. Barsotti, J. Bartlett, M. A. Barton, I. Bartos, R. Bassiri, J. C. Batch, C. Baune, B. Behnke, A. S. Bell, C. Bell, M. Benacquista, J. Bergman, G. Bergmann, C. P. L. Berry, J. Betzwieser, S. Bhagwat, R. Bhandare, I. A. Bilenko, G. Billingsley, J. Birch, S. Biscans, C. Biwer, J. K. Blackburn, L. Blackburn, C. D. Blair, D. Blair, O. Bock, T. P. Bodiya, P. Bojtos, C. Bond, R. Bork, M. Born, S. Bose, P. R. Brady, V. B. Braginsky, J. E. Brau, D. O. Bridges, M. Brinkmann, A. F. Brooks, D. A. Brown, D. D. Brown, N. M. Brown, S. Buchman, A. Buikema, A. Buonanno, L. Cadonati, J. C. Bustillo, J. B. Camp, K. C. Cannon, J. Cao, C. D. Capano, S. Caride, S. Caudill, M. Cavagliá, C. Cepeda, R. Chakraborty, T. Chalermsongsak, S. J. Chamberlin, S. Chao, P. Charlton, Y. Chen, H. S. Cho, M. Cho, J. H. Chow, N. Christensen, Q. Chu, S. Chung, G. Ciani, F. Clara, J. A. Clark, C. Collette, L. Cominsky, M. Constancio, D. Cook, T. R. Corbitt, N. Cornish, A. Corsi, C. A. Costa, M. W. Coughlin, S. Countryman, P. Couvares, D. M. Coward, M. J. Cowart, D. C. Coyne, R. Coyne, K. Craig, J. D. E. Creighton, T. D. Creighton, J. Cripe, S. G. Crowder, A. Cumming, L. Cunningham, C. Cutler, K. Dahl, T. D. Canton, M. Damjanic, S. L. Danilishin, K. Danzmann, L. Dartez, I. Dave, H. Daveloza, G. S. Davies, E. J. Daw, D. DeBra, W. D. Pozzo, T. Denker, T. Dent, V. Dergachev, R. T. DeRosa, R. DeSalvo, S. Dhurandhar, M. Díaz, I. D. Palma, G. Dojcinoski, E. Dominguez, F. Donovan, K. L. Dooley, S. Doravari, R. Douglas, T. P. Downes, J. C. Driggers, Z. Du, S. Dwyer, T. Eberle, T. Edo, M. Edwards, M. Edwards, A. Effler, H.-B. Eggenstein, P. Ehrens, J. Eichholz, S. S. Eikenberry, R. Essick, T. Etzel, M. Evans, T. Evans, M. Factourovich, S. Fairhurst, X. Fan, Q. Fang, B. Farr, W. M. Farr, M. Favata, M. Fays, H. Fehrmann, M. M. Fejer, D. Feldbaum, E. C. Ferreira, R. P. Fisher, Z. Frei, A. Freise, R. Frey, T. T. Fricke, P. Fritschel, V. V. Frolov, S. Fuentes-Tapia, P. Fulda, M. Fyffe, J. R. Gair, S. Gaonkar, N. Gehrels, L. Á. Gergely, J. A. Giaime, K. D. Giardina, J. Gleason, E. Goetz, R. Goetz, L. Gondan, G. González, N. Gordon, M. L. Gorodetsky, S. Gossan, S. Goßler, C. Gräf, P. B. Graff, A. Grant, S. Gras, C. Gray, R. J. S. Greenhalgh, A. M. Gretarsson, H. Grote, S. Grunewald, C. J. Guido, X. Guo, K. Gushwa, E. K. Gustafson, R. Gustafson, J. Hacker, E. D. Hall, G. Hammond, M. Hanke, J. Hanks, C. Hanna, M. D. Hannam, J. Hanson, T. Hardwick, G. M. Harry, I. W. Harry, M. Hart, M. T. Hartman, C.-J. Haster, K. Haughian, S. Hee, M. Heintze, G. Heinzel, M. Hendry, I. S. Heng, A. W. Heptonstall, M. Heurs, M. Hewitson, S. Hild, D. Hoak, K. A. Hodge, S. E. Hollitt, K. Holt, P. Hopkins, D. J. Hosken, J. Hough, E. Houston, E. J. Howell, Y. M. Hu, E. Huerta, B. Hughey, S. Husa, S. H. Huttner, M. Huynh, T. Huynh-Dinh, A. Idrisy, N. Indik, D. R. Ingram, R. Inta, G. Islas, J. C. Isler, T. Isogai, B. R. Iyer, K. Izumi, M. Jacobson, H. Jang, S. Jawahar, Y. Ji, F. Jiménez-Forteza, W. W. Johnson, D. I. Jones, R. Jones, L. Ju, K. Haris, V. Kalogera, S. Kandhasamy, G. Kang, J. B. Kanner, E. Katsavounidis, W. Katzman, H. Kaufer, S. Kaufer, T. Kaur, K. Kawabe, F. Kawazoe, G. M. Keiser, D. Keitel, D. B. Kelley, W. Kells, D. G. Keppel, J. S. Key, A. Khalaidovski, F. Y. Khalili, E. A. Khazanov, C. Kim, K. Kim, N. G. Kim, N. Kim, Y.-M. Kim, E. J. King, P. J. King, D. L. Kinzel, J. S. Kissel, S. Klimenko, J. Kline, S. Koehlenbeck, K. Kokeyama, V. Kondrashov, M. Korobko, W. Z. Korth, D. B. Kozak, V. Kringel, B. Krishnan, C. Krueger, G. Kuehn, A. Kumar, P. Kumar, L. Kuo, M. Landry, B. Lantz, S. Larson, P. D. Lasky, A. Lazzarini, C. Lazzaro, J. Le, P. Leaci, S. Leavey, E. O. Lebigot, C. H. Lee, H. K. Lee, H. M. Lee, J. R. Leong, Y. Levin, B. Levine, J. Lewis, T. G. F. Li, K. Libbrecht, A. Libson, A. C. Lin, T. B. Littenberg, N. A. Lockerbie, V. Lockett, J. Logue, A. L. Lombardi, M. Lormand, J. Lough, M. J. Lubinski, H. Lück, A. P. Lundgren, R. Lynch, Y. Ma, J. Macarthur, T. MacDonald, B. Machenschalk, M. MacInnis, D. M. Macleod, F. Magaña-Sandoval, R. Magee, M. Mageswaran, C. Maglione, K. Mailand, I. Mandel, V. Mandic, V. Mangano, G. L. Mansell, S. Márka, Z. Márka, A. Markosyan, E. Maros, I. W. Martin, R. M. Martin, D. Martynov, J. N. Marx, K. Mason, T. J. Massinger, F. Matichard, L. Matone, N. Mavalvala, N. Mazumder, G. Mazzolo, R. McCarthy, D. E. McClelland, S. McCormick, S. C. McGuire, G. McIntyre, J. McIver, K. McLin, S. McWilliams, G. D. Meadors, M. Meinders, A. Melatos, G. Mendell, R. A. Mercer, S. Meshkov, C. Messenger, P. M. Meyers, H. Miao, H. Middleton, E. E. Mikhailov, A. Miller, J. Miller, M. Millhouse, J. Ming, S. Mirshekari, C. Mishra, S. Mitra, V. P. Mitrofanov, G. Mitselmakher, R. Mittleman, B. Moe, S. D. Mohanty, S. R. P. Mohapatra, B. Moore, D. Moraru, G. Moreno, S. R. Morriss, K. Mossavi, C. M. Mow-Lowry, C. L. Mueller, G. Mueller, S. Mukherjee, A. Mullavey, J. Munch, D. Murphy, P. G. Murray, A. Mytidis, T. Nash, R. K. Nayak, V. Necula, K. Nedkova, G. Newton, T. Nguyen, A. B. Nielsen, S. Nissanke, A. H. Nitz, D. Nolting, M. E. N. Normandin, L. K. Nuttall, E. Ochsner, J. O'Dell, E. Oelker, G. H. Ogin, J. J. Oh, S. H. Oh, F. Ohme, P. Oppermann, R. Oram, B. O'Reilly, W. Ortega, R. O'Shaughnessy, C. Osthelder, C. D. Ott, D. J. Ottaway, R. S. Ottens, H. Overmier, B. J. Owen, C. Padilla, A. Pai, S. Pai, O. Palashov, A. Pal-Singh, H. Pan, C. Pankow, F. Pannarale, B. C. Pant, M. A. Papa, H. Paris, Z. Patrick, M. Pedraza, L. Pekowsky, A. Pele, S. Penn, A.

Optics EXPRESS

Perreca, M. Phelps, V. Pierro, I. M. Pinto, M. Pitkin, J. Poeld, A. Post, A. Poteomkin, J. Powell, J. Prasad, V. Predoi, S. Premachandra, T. Prestegard, L. R. Price, M. Principe, S. Privitera, R. Prix, L. Prokhorov, O. Puncken, M. Pürrer, J. Qin, V. Quetschke, E. Quintero, G. Quiroga, R. Quitzow-James, F. J. Raab, D. S. Rabeling, H. Radkins, P. Raffai, S. Raja, G. Rajalakshmi, M. Rakhmanov, K. Ramirez, V. Raymond, C. M. Reed, S. Reid, D. H. Reitze, O. Reula, K. Riles, N. A. Robertson, R. Robie, J. G. Rollins, V. Roma, J. D. Romano, G. Romanov, J. H. Romie, S. Rowan, A. Rüdiger, K. Ryan, S. Sachdev, T. Sadecki, L. Sadeghian, M. Saleem, F. Salemi, L. Sammut, V. Sandberg, J. R. Sanders, V. Sannibale, I. Santiago-Prieto, B. S. Sathyaprakash, P. R. Saulson, R. Savage, A. Sawadsky, J. Scheuer, R. Schilling, P. Schmidt, R. Schnabel, R. M. S. Schofield, E. Schreiber, D. Schuette, B. F. Schutz, J. Scott, S. M. Scott, D. Sellers, A. S. Sengupta, A. Sergeev, G. Serna, A. Sevigny, D. A. Shaddock, M. S. Shahriar, M. Shaltev, Z. Shao, B. Shapiro, P. Shawhan, D. H. Shoemaker, T. L. Sidery, X. Siemens, D. Sigg, A. D. Silva, D. Simakov, A. Singer, L. Singer, R. Singh, A. M. Sintes, B. J. J. Slagmolen, J. R. Smith, M. R. Smith, R. J. E. Smith, N. D. Smith-Lefebvre, E. J. Son, B. Sorazu, T. Souradeep, A. Staley, J. Stebbins, M. Steinke, J. Steinlechner, S. Steinlechner, D. Steinmeyer, B. C. Stephens, S. Steplewski, S. Stevenson, R. Stone, K. A. Strain, S. Strigin, R. Sturani, A. L. Stuver, T. Z. Summerscales, P. J. Sutton, M. Szczepanczyk, G. Szeifert, D. Talukder, D. B. Tanner, M. Tápai, S. P. Tarabrin, A. Taracchini, R. Taylor, G. Tellez, T. Theeg, M. P. Thirugnanasambandam, M. Thomas, P. Thomas, K. A. Thorne, K. S. Thorne, E. Thrane, V. Tiwari, C. Tomlinson, C. V. Torres, C. I. Torrie, G. Traylor, M. Tse, D. Tshilumba, D. Ugolini, C. S. Unnikrishnan, A. L. Urban, S. A. Usman, H. Vahlbruch, G. Vajente, G. Valdes, M. Vallisneri, A. A. van Veggel, S. Vass, R. Vaulin, A. Vecchio, J. Veitch, P. J. Veitch, K. Venkateswara, R. Vincent-Finley, S. Vitale, T. Vo, C. Vorvick, W. D. Vousden, S. P. Vyatchanin, A. R. Wade, L. Wade, M. Wade, M. Walker, L. Wallace, S. Walsh, H. Wang, M. Wang, X. Wang, R. L. Ward, J. Warner, M. Was, B. Weaver, M. Weinert, A. J. Weinstein, R. Weiss, T. Welborn, L. Wen, P. Wessels, T. Westphal, K. Wette, J. T. Whelan, S. E. Whitcomb, D. J. White, B. F. Whiting, C. Wilkinson, L. Williams, R. Williams, A. R. Williamson, J. L. Willis, B. Willke, M. Wimmer, W. Winkler, C. C. Wipf, H. Wittel, G. Woan, J. Worden, S. Xie, J. Yablon, I. Yakushin, W. Yam, H. Yamamoto, C. C. Yancey, Q. Yang, M. Zanolin, F. Zhang, L. Zhang, M. Zhang, Y. Zhang, C. Zhao, M. Zhou, X. J. Zhu, M. E. Zucker, S. Zuraw, and J. Zweizig, "Advanced LIGO," Classical Quantum Gravity **32**(7), 074001 (2015).

3. F. Acernese, M. Agathos, K. Agatsuma, D. Aisa, N. Allemandou, A. Allocca, J. Amarni, P. Astone, G. Balestri, G. Ballardin, F. Barone, J.-P. Baronick, M. Barsuglia, A. Basti, F. Basti, T. S. Bauer, V. Bavigadda, M. Bejger, M. G. Beker, C. Belczynski, D. Bersanetti, A. Bertolini, M. Bitossi, M. A. Bizouard, S. Bloemen, M. Blom, M. Boer, G. Bogaert, D. Bondi, F. Bondu, L. Bonelli, R. Bonnand, V. Boschi, L. Bosi, T. Bouedo, C. Bradaschia, M. Branchesi, T. Briant, A. Brillet, V. Brisson, T. Bulik, H. J. Bulten, D. Buskulic, C. Buy, G. Cagnoli, E. Calloni, C. Campeggi, B. Canuel, F. Carbognani, F. Cavalier, R. Cavalieri, G. Cella, E. Cesarini, E. Chassande-Mottin, A. Chincarini, A. Chiummo, S. Chua, F. Cleva, E. Coccia, P.-F. Cohadon, A. Colla, M. Colombini, A. Conte, J.-P. Coulon, E. Cuoco, A. Dalmaz, S. D'Antonio, V. Dattilo, M. Davier, R. Day, G. Debreczeni, J. Degallaix, S. Deléglise, W. D. Pozzo, H. Dereli, R. D. Rosa, L. D. Fiore, A. D. Lieto, A. D. Virgilio, M. Doets, V. Dolique, M. Drago, M. Ducrot, G. Endrőczi, V. Fafone, S. Farinon, I. Ferrante, F. Ferrini, F. Fidecaro, I. Fiori, R. Flaminio, J.-D. Fournier, S. Franco, S. Frasca, F. Frasconi, L. Gammaitoni, F. Garufi, M. Gaspard, A. Gatto, G. Gemme, B. Gendre, E. Genin, A. Gennai, S. Ghosh, L. Giacobone, A. Giazotto, R. Gouaty, M. Granata, G. Greco, P. Groot, G. M. Guidi, J. Harms, A. Heidmann, H. Heitmann, P. Hello, G. Hemming, E. Hennes, D. Hofman, P. Jaranowski, R. J. G. Jonker, M. Kasprzack, F. Kéfélian, I. Kowalska, M. Kraan, A. Królak, A. Kutynia, C. Lazzaro, M. Leonardi, N. Leroy, N. Letendre, T. G. F. Li, B. Lieunard, M. Lorenzini, V. Loriette, G. Losurdo, C. Magazzù, E. Majorana, I. Maksimovic, V. Malvezzi, N. Man, V. Mangano, M. Mantovani, F. Marchesoni, F. Marion, J. Marque, F. Martelli, L. Martellini, A. Masserot, D. Meacher, J. Meidam, F. Mezzani, C. Michel, L. Milano, Y. Minenkov, A. Moggi, M. Mohan, M. Montani, N. Morgado, B. Mours, F. Mul, M. F. Nagy, I. Nardecchia, L. Naticchioni, G. Nelemans, I. Neri, M. Neri, F. Nocera, E. Pacaud, C. Palomba, F. Paoletti, A. Paoli, A. Pasqualetti, R. Passaquieti, D. Passuello, M. Perciballi, S. Petit, M. Pichot, F. Piergiovanni, G. Pillant, A. Piluso, L. Pinard, R. Poggiani, M. Prijatelj, G. A. Prodi, M. Punturo, P. Puppo, D. S. Rabeling, I. Rácz, P. Rapagnani, M. Razzano, V. Re, T. Regimbau, F. Ricci, F. Robinet, A. Rocchi, L. Rolland, R. Romano, D. Rosińska, P. Ruggi, E. Saracco, B. Sassolas, F. Schimmel, D. Sentenac, V. Sequino, S. Shah, K. Siellez, N. Straniero, B. Swinkels, M. Tacca, M. Tonelli, F. Travasso, M. Turconi, G. Vajente, N. van Bakel, M. van Beuzekom, J. F. J. van den Brand, C. V. D. Broeck, M. V. van der Sluys, J. van Heijningen, M. Vasúth, G. Vedovato, J. Veitch, D. Verkindt, F. Vetrano, A. Viceré, J.-Y. Vinet, G. Visser, H. Vocca, R. Ward, M. Was, L.-W. Wei, M. Yvert, A. Z. żny, and J.-P. Zendri, "Advanced Virgo: a second-generation interferometric gravitational wave detector," Classical Quantum Gravity **32**(2), 024001 (2015).
4. T. Nazarova, C. Lisdat, F. Riehle, and U. Sterr, "Low-frequency-noise diode laser for atom interferometry," J. Opt. Soc. Am. B **25**(10), 1632–1638 (2008).
5. C. Eisele, A. Y. Nevsky, and S. Schiller, "Laboratory test of the isotropy of light propagation at the 10^{-17} level," Phys. Rev. Lett. **103**(9), 090401 (2009).
6. T. Kane and R. Byer, "Monolithic, Unidirectional Single-Mode Nd:YAG Ring Laser," Opt. Lett. **10**(2), 65–67 (1985).
7. B. Willke, "Stabilized lasers for advanced gravitational wave detectors," Laser Photonics Rev. **4**(6), 780–794 (2010).
8. N. Bode, J. Briggs, X. Chen, M. Frede, P. Fritschel, M. Fyffe, E. Gustafson, M. Heintze, P. King, J. Liu, J. Oberling, R. L. Savage, A. Spencer, and B. Willke, "Advanced LIGO Laser Systems for O3 and Future Observation Runs," Galaxies **8**(4), 84 (2020).
9. M. Punturo, M. Abernathy, F. Acernese, B. Allen, N. Andersson, K. Arun, F. Barone, B. Barr, M. Barsuglia, M. Beker, N. Beveridge, S. Birindelli, S. Bose, L. Bosi, S. Braccini, C. Bradaschia, T. Bulik, E. Calloni, G. Cella, E. C.

Optics EXPRESS

Mottin, S. Chelkowski, A. Chincarini, J. Clark, E. Coccia, C. Colacino, J. Colas, A. Cumming, L. Cunningham, E. Cuoco, S. Danilishin, K. Danzmann, G. D. Luca, R. D. Salvo, T. Dent, R. D. Rosa, L. D. Fiore, A. D. Virgilio, M. Doets, V. Fafone, P. Falferi, R. Flaminio, J. Franc, F. Frasconi, A. Freise, P. Fulda, J. Gair, G. Gemme, A. Gennai, A. Giazotto, K. Glampedakis, M. Granata, H. Grote, G. Guidi, G. Hammond, M. Hannam, J. Harms, D. Heinert, M. Hendry, I. Heng, E. Hennes, S. Hild, J. Hough, S. Husa, S. Huttner, G. Jones, F. Khalili, K. Kokeyama, K. Kokkotas, B. Krishnan, M. Lorenzini, H. Lück, E. Majorana, I. Mandel, V. Mandic, I. Martin, C. Michel, Y. Minenkov, N. Morgado, S. Mosca, B. Mours, H. Müller-Ebhardt, P. Murray, R. Nawrodt, J. Nelson, R. Oshaughnessy, C. D. Ott, C. Palomba, A. Paoli, G. Parguez, A. Pasqualetti, R. Passaquieti, D. Passuello, L. Pinard, R. Poggiani, P. Popolizio, M. Prato, P. Puppo, D. Rabeling, P. Rapagnani, J. Read, T. Regimbau, H. Rehbein, S. Reid, L. Rezzolla, F. Ricci, F. Richard, A. Rocchi, S. Rowan, A. Rüdiger, B. Sassolas, B. Sathyaprakash, R. Schnabel, C. Schwarz, P. Seidel, A. Sintes, K. Somiya, F. Speirits, K. Strain, S. Strigin, P. Sutton, S. Tarabrin, A. Thüring, J. van den Brand, C. van Leewen, M. van Veggel, C. van den Broeck, A. Vecchio, J. Veitch, F. Vetrano, A. Vicere, S. Vyatchanin, B. Willke, G. Woan, P. Wolfango, and K. Yamamoto, "The Einstein Telescope: a third-generation gravitational wave observatory," Classical Quantum Gravity **27**(19), 194002 (2010).

10. R. X. Adhikari, P. Ajith, Y. Chen, J. A. Clark, V. Dergachev, N. V. Fotopoulos, S. E. Gossan, I. Mandel, M. Okounkova, V. Raymond, and J. S. Read, "Astrophysical science metrics for next-generation gravitational-wave detectors," Classical Quantum Gravity **36**(24), 245010 (2019).
11. F. Meylahn and B. Willke, "Characterization of laser systems at 1550 nm wavelength for future gravitational wave detectors," Instruments **6**(1), 15 (2022).
12. D. P. Kapasi, J. Eichholz, T. McRae, R. L. Ward, B. J. J. Slagmolen, S. Legge, K. S. Hardman, P. A. Altin, and D. E. McClelland, "Tunable narrow-linewidth laser at 2μm wavelength for gravitational wave detector research," Opt. Express **28**(3), 3280–3288 (2020).
13. S. Bennetts, G. D. McDonald, K. S. Hardman, J. E. Debs, C. C. N. Kuhn, J. D. Close, and N. P. Robins, "External cavity diode lasers with 5khz linewidth and 200nm tuning range at 1.55μm and methods for linewidth measurement," Opt. Express **22**(9), 10642–10654 (2014).
14. H. Stoehr, F. Mensing, J. Helmcke, and U. Sterr, "Diode laser with 1 Hz linewidth," Opt. Lett. **31**(6), 736–738 (2006).
15. P. Kwee, C. Bogan, K. Danzmann, M. Frede, H. Kim, P. King, J. Pold, O. Puncken, R. Savage, F. Seifert, P. Weßels, L. Winkelmann, and B. Willke, "Stabilized High-Power Laser System for the Gravitational Wave Detector Advanced LIGO," Opt. Express **20**(10), 10617–10634 (2012).
16. S. Hild, M. Abernathy, F. Acernese, P. Amaro-Seoane, N. Andersson, K. Arun, F. Barone, B. Barr, M. Barsuglia, M. Beker, N. Beveridge, S. Birindelli, S. Bose, L. Bosi, S. Braccini, C. Bradaschia, T. Bulik, E. Calloni, G. Cella, E. C. Mottin, S. Chelkowski, A. Chincarini, J. Clark, E. Coccia, C. Colacino, J. Colas, A. Cumming, L. Cunningham, E. Cuoco, S. Danilishin, K. Danzmann, R. D. Salvo, T. Dent, R. D. Rosa, L. D. Fiore, A. D. Virgilio, M. Doets, V. Fafone, P. Falferi, R. Flaminio, J. Franc, F. Frasconi, A. Freise, D. Friedrich, P. Fulda, J. Gair, G. Gemme, E. Genin, A. Gennai, A. Giazotto, K. Glampedakis, C. Gräf, M. Granata, H. Grote, G. Guidi, A. Gurkovsky, G. Hammond, M. Hannam, J. Harms, D. Heinert, M. Hendry, I. Heng, E. Hennes, J. Hough, S. Husa, S. Huttner, G. Jones, F. Khalili, K. Kokeyama, K. Kokkotas, B. Krishnan, T. G. F. Li, M. Lorenzini, H. Lück, E. Majorana, I. Mandel, V. Mandic, M. Mantovani, I. Martin, C. Michel, Y. Minenkov, N. Morgado, S. Mosca, B. Mours, H. Müller-Ebhardt, P. Murray, R. Nawrodt, J. Nelson, R. Oshaughnessy, C. D. Ott, C. Palomba, A. Paoli, G. Parguez, A. Pasqualetti, R. Passaquieti, D. Passuello, L. Pinard, W. Plastino, R. Poggiani, P. Popolizio, M. Prato, M. Punturo, P. Puppo, D. Rabeling, P. Rapagnani, J. Read, T. Regimbau, H. Rehbein, S. Reid, F. Ricci, F. Richard, A. Rocchi, S. Rowan, A. Rüdiger, L. Santamaría, B. Sassolas, B. Sathyaprakash, R. Schnabel, C. Schwarz, P. Seidel, A. Sintes, K. Somiya, F. Speirits, K. Strain, S. Strigin, P. Sutton, S. Tarabrin, A. Thüring, J. van den Brand, M. van Veggel, C. van den Broeck, A. Vecchio, J. Veitch, F. Vetrano, A. Vicere, S. Vyatchanin, B. Willke, G. Woan, and K. Yamamoto, "Sensitivity studies for third-generation gravitational wave observatories," Classical Quantum Gravity **28**(9), 094013 (2011).
17. "Pure Photonics," https://www.pure-photonics.com/.
18. P. Kwee and B. Willke, "Automatic Laser Beam Characterization of Monolithic Nd:YAG Nonplanar Ring Lasers," Appl. Opt. **47**(32), 6022–6032 (2008).
19. C. Henry, "Phase noise in semiconductor lasers," J. Lightwave Technol. **4**(3), 298–311 (1986).
20. M. Fukuda, T. Hirono, T. Kurosaki, and F. Kano, "1/f noise behavior in semiconductor laser degradation," IEEE Photonics Technol. Lett. **5**(10), 1165–1167 (1993).
21. B. Bartolo, C. Kirkendall, V. Kupershmidt, and S. Siala, "Achieving narrow linewidth, low phase noise external cavity semiconductor lasers through the reduction of 1/f noise - art. no. 61330i," Proc. SPIE **6133**, 61330I (2006).
22. A. Dandridge and L. Goldberg, "Current-induced frequency modulation in diode lasers," Electron. Lett. **18**(7), 302–304 (1982).
23. "Extremely Low Thermal Expansion Glass Ceramic ZERODUR," https://www.schott.com/advanced_optics/english/products/optical-materials/zerodur-extremely-low-expansion-glass-ceramic/zerodur/index.html.
24. R. Drever, J. Hall, F. Kowalski, J. Hough, G. Ford, A. Munley, and H. Ward, "Laser Phase and Frequency Stabilization Using an Optical Resonator," Appl. Phys. B **31**(2), 97–105 (1983).
25. K. Numata, A. Kemery, and J. Camp, "Thermal-noise limit in the frequency stabilization of lasers with rigid cavities," Phys. Rev. Lett. **93**(25), 250602 (2004).
26. K. Arai, "OMC thermal noise calculation," https://dcc.ligo.org/LIGO-G1800149/public.

Optics EXPRESS

27. M. Notcutt, L.-S. Ma, A. D. Ludlow, S. M. Foreman, J. Ye, and J. L. Hall, "Contribution of thermal noise to frequency stability of rigid optical cavity via hertz-linewidth lasers," Phys. Rev. A **73**(3), 031804 (2006).
28. J. Hough, H. Ward, G. A. Kerr, N. L. MacKenzie, B. J. Meers, G. P. Newton, D. I. Robertson, N. A. Robertson, and R. Schilling, "The stabilisation of lasers for interferometric gravitational wave detectors," in *The Detection of Gravitational Waves*, D. Blair, ed. (Cambridge University Press, 1991), p. 329–352.
29. E. M. Kerwin, "Damping of Flexural Waves by a Constrained Viscoelastic Layer," J. Acoust. Soc. Am. **31**(7), 952–962 (1959).
30. A. Ryou and J. Simon, "Active cancellation of acoustical resonances with an FPGA FIR filter," Rev. Sci. Instrum. **88**(1), 013101 (2017).
31. G. Franklin, J. Powell, and M. Workman, *Digital Control of Dynamic Systems* (Prentice Hall, 1997).
32. J. Kennedy and R. Eberhart, "Particle swarm optimization," in *Proceedings of ICNN'95 - International Conference on Neural Networks*, vol. 4 (1995), pp. 1942–1948 vol.4.
33. E. Mezura-Montes and C. A. Coello Coello, "Constraint-handling in nature-inspired numerical optimization: Past, present and future," Swarm Evol. Comput. **1**(4), 173–194 (2011).